

## **A MICROSTRIP-FED MULTIBAND SPIRAL RING MONOPOLE ANTENNA WITH IMPROVED RADIATION CHARACTERISTICS AT HIGHER RESONANT FREQUENCIES**

**Fu-Shun Zhang, Yang-Tao Wan<sup>\*</sup>, Dan Yu, and Bing Ye**

National Laboratory of Science and Technology on Antennas and Microwaves, Xidian University, Xi'an, Shaanxi 710071, P. R. China

**Abstract**—A novel approach for the design of a compact multiband monopole antenna for improving radiation characteristics at higher resonant frequencies is presented. The proposed structure consists of a conventional printed monopole loaded with spiral ring resonators and fed by microstrip. When at higher resonant frequency, the electrical length of the conventional monopole antennas is relatively large and the surface currents distribute on the patch periodically which will degrade the omnidirectional property. To achieve good radiation characteristics at the upper bands, two spiral ring strips are inserted into the microstrip line on the different layer and connected through via hole. Thus, the direction of surface currents on the spiral ring strips changes with the alteration of spiral structure and their effects on the radiation pattern are reduced. The radiation pattern is mainly contributed by the surface current on the microstrip line and very good stable radiation pattern can be obtained within all the operating bands. In comparison to the previous printed strip monopole structures, the miniaturized Antenna dimension is only about  $28\text{ mm} \times 20\text{ mm} \times 1\text{ mm}$ . The experimental results show that the proposed antenna can provide operating bands which meet the required bandwidths specification of 2.4/5.2 GHz WLAN and 3.5 GHz WiMAX standard. Detailed design considerations of the proposed Antenna are described, and both the simulated and measured results of the proposed Antenna are also presented and discussed.

---

*Received 7 May 2013, Accepted 6 June 2013, Scheduled 18 June 2013*

\* Corresponding author: Yang-Tao Wan (wanyangtao@163.com).

## 1. INTRODUCTION

With the rapid development of modern wireless communication system, antenna design has returned to focus on multiband and simple structures that can be easy to fabricate. To adapt to complicated and diverse WLAN and WiMAX environment, a large number of such antennas have been proposed [1–6]. Though the proposed antennas have good characteristics for both WLAN and WiMAX applications, they are complicated in structures and large in size. In [1], slots have been used to generate extra resonances controlled by varying the slot geometry. Differently, the multiband behavior has been obtained in [2–4] by extending the geometry of a reference shape adding strips, stubs or parasitic elements. In [5, 6], two or more branches, and even fractal patterns are added to the monopole design to excite multiple resonant bands. Some compact antennas [7–12] have also been proposed. Different techniques have been applied to antenna design to make the structures simple and easy to fabricate. For example, in [7–9], CPW-fed or microstrip-fed structures can minimize the antenna size. In [10], a hybrid ring fractal printed monopole with semiellipse ground plane can have a very compact size and good impedance characteristics. Capacitive and inductive loading or meta-material loading are also seen in [11, 12] to reduce the antenna size and increase the Antenna bandwidth.

However, there is a limit of these antennas to obtain stably good radiation patterns within all these operating bands especially at the upper bands. It is well known that the electrical length of these antennas in the upper bands is relatively large, often several times of the wavelength, and the surface currents distribute on the patch periodically. The combined action of the forward and reverse surface currents will tilt the direction of maximum radiation in the  $E$ -plane and degrade the omnidirectional property in the  $H$ -plane. Therefore, the radiated power of the conventional antennas decreases a lot, which degrades the performance of these antennas in the wireless communication.

In this paper, a compact microstrip-fed multiband monopole antenna based on spiral ring resonators which covers 2.4/5.2 GHz WLAN and 3.5 GHz WiMAX is proposed. It comprises two spiral ring strips on the different layer of the substrate which are connected by via. Due to the introduction of the spiral ring strips, the direction of surface currents on the spiral ring strips changes with the alteration of spiral structure and their effects on the radiation pattern are reduced. Thus, the maximum radiated direction in  $E$ -plane is stable and omnidirectional property in the  $H$ -plane is also very good within

the desired frequency bands. In addition, the spiral ring structure extends the route of the surface currents and miniaturizes the size of the proposed Antenna. Both simulation and measurement results were provided to validate the antenna performance.

The paper is organized in the following sections. Section 2 contains the basic theory and the computational method. Section 3 contains the antenna geometry. Analysis of the calculated and measured results of the prototype are presented and discussed in Section 4, followed by a conclusion of this work.

## 2. THEORY AND METHOD

It is well known that the frequencies of the ring resonators are determined by their dimensions, i.e., the resonant frequencies are generally directly proportional to their diameters. In [13], a simple transmission-line model method is used to calculate the frequency modes of ring resonators of any general shape. The resonant frequencies and guided wavelengths of a one-port ring resonators using transmission-line model method can be defined by

$$2\pi r = n \frac{\lambda_g}{2}, \quad n = 1, 2, 3 \dots \quad (1)$$

$$f_0 = \frac{nc}{2l\sqrt{\varepsilon_{eff}}}, \quad n = 1, 2, 3 \dots \quad (2)$$

where  $\lambda_g$  is the guided wavelength,  $r$  the radius of the ring resonator,  $n$  the mode number,  $f_0$  the resonant frequencies,  $l$  the total length of the ring resonator ( $l = 2\pi r$ ),  $\varepsilon_{eff}$  the effective dielectric constant, and  $c$  the speed of light in free space.

In the same way, the transmission-line model method can also be used to calculate the frequency modes of spiral ring resonators shown in Figure 1(b). The frequency modes are approximately given as

$$f_0 = \frac{nc}{2l_{total}\sqrt{\varepsilon_{eff}}}, \quad n = 1, 2, 3 \dots \quad (3)$$

where  $l_{total}$  is the total effective length of the spiral ring resonators including a part of strip line.

From the Eq. (3), we can figure out the resonant frequencies of the proposed antenna approximately. As we all know, the resonant frequencies modes of the conventional ring resonators have a correlated relationship, and the frequency ratio is fixed. In order to cover 2.4/5.2 GHz WLAN and 3.5 GHz WiMAX, the gap  $d$  between the inner and outer spiral rings is slightly adjusted to change the frequency ratio of these operating frequency bands. The effect of the gap  $d$  on the frequency ratio is studied in Section 4.2.

To verify the theory and the computational method, simulation results of the proposed antenna are performed in the following section.

### 3. ANTENNA STRUCTURE AND DESIGN

The design starts with the conventional microstrip-fed monopole named Antenna A, shown in Figure 1(a). Two spiral ring strips are then inserted on it on the different layer to form Antenna B, shown in Figure 1(b). This section details the antenna design procedure.

The conventional monopole antenna is shown in Figure 1(a), with the  $xz$ -plane and  $yz$ -plane referred to as the  $E$ - and  $H$ -planes, respectively. The size of Antenna A is  $98 \text{ mm} \times 20 \text{ mm}$  with substrate thickness ( $h$ ) of  $1 \text{ mm}$  and dielectric constant ( $\epsilon_r$ ) equal to  $2.65$ . The proper parameters for the conventional monopole antenna configuration were:  $L = 98 \text{ mm}$ ,  $W = 20 \text{ mm}$ ,  $W_1 = 2 \text{ mm}$ ,  $L_1 = 10 \text{ mm}$ .

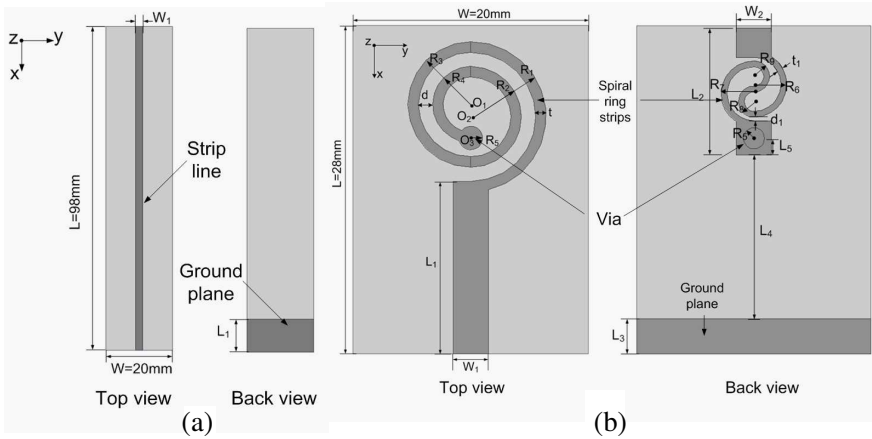


**Figure 1.** The structural configurations of the conventional monopole Antenna and the proposed Antenna. (a) Antenna A; (b) Antenna B.

In comparison to the conventional monopole structure, the proposed antenna has a more compact size of  $28 \text{ mm} \times 20 \text{ mm} \times 1 \text{ mm}$  due to the spiral ring structure extends the route of the surface currents. The configuration of Antenna B loaded with two spiral ring strips is illustrated in Figure 1(b). The size of the ground plane is  $10 \text{ mm} \times 20 \text{ mm}$  with substrate thickness ( $h$ ) of  $1 \text{ mm}$  and dielectric constant ( $\epsilon_r$ ) equal to  $2.65$ . The spiral ring resonator on the top side is composed of four semi-circle rings. Both the right side and left side two semi-circle rings are concentric and separated by a gap  $d$ . The

gap  $d$  plays a vital role to the frequency ratio of the two operating frequency bands. The other spiral ring resonator on the rear side is also composed of four semi-circle rings with a different center.  $R_1, R_2, R_3, R_4, R_6, R_7, R_8$  and  $R_9$  are the radius of these eight semi-circle rings, respectively. Two spiral ring strips are connected by via with a radius of  $R_5$ . The widths of the metal lines of these rings are  $t = 0.9\text{ mm}$  and  $t_1 = 0.5\text{ mm}$  on the different sides. A microstrip line with a width of  $W_1 = 3\text{ mm}$  is used to feed the antenna. The proper parameters for Antenna B configuration were:  $L = 28\text{ mm}$ ,  $W = 20\text{ mm}$ ,  $L_1 = 14.7\text{ mm}$ ,  $W_1 = 3\text{ mm}$ ,  $L_2 = 10.8\text{ mm}$ ,  $L_3 = 3\text{ mm}$ ,  $L_4 = 14\text{ mm}$ ,  $L_5 = 14.5\text{ mm}$ ,  $R_1 = 6.4\text{ mm}$ ,  $R_2 = 4.3\text{ mm}$ ,  $R_3 = 5.35\text{ mm}$ ,  $R_4 = 3.25\text{ mm}$ ,  $R_5 = 0.9\text{ mm}$ ,  $t = 0.9\text{ mm}$ ,  $R_6 = 2.7\text{ mm}$ ,  $R_7 = 2.7\text{ mm}$ ,  $R_8 = 1.275\text{ mm}$ ,  $R_9 = 1.275\text{ mm}$ ,  $t_1 = 0.5\text{ mm}$ ,  $d = 1.2\text{ mm}$ ,  $d_1 = 0.3\text{ mm}$ .

#### 4. RESULTS AND DISCUSSION

##### 4.1. Comparison of Reflection Coefficient ( $S_{11}$ ) between Conventional Monopole Antenna and the Proposed Antenna

Figure 2 shows the simulated  $|S_{11}|$  of the conventional monopole antenna (Antenna A) and the proposed antenna (Antenna B). Antenna A is, for the sake of comparison, designed to operate at the same fundamental resonant frequency as Antenna B.

From Figure 2, we can see that Antenna A has four frequency modes in the frequency range from 1 GHz to 6 GHz, while Antenna B

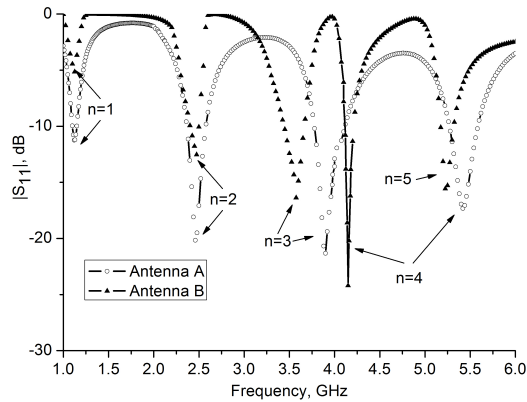


**Figure 2.** Comparison of the simulated  $|S_{11}|$  between Antenna A and Antenna B.

possesses five frequency modes. The first band of Antenna A is located at 1.12 GHz with the impedance bandwidth of about 50 MHz. The second resonant mode extends from 2.37 to 2.55 GHz with the impedance bandwidth of about 180 MHz, and the third band stretches from 3.74 to 4.06 GHz whose impedance bandwidth is 320 MHz. The fourth band, which begins from 5.27 to 5.57 GHz, has a bandwidth of 300 MHz. Antenna B resonates at 1.1 GHz which is satisfied with frequency mode number  $n$  equal to 1. The reflection coefficient at the first band is  $-5.4$  dB which is worse than  $-10$  dB due to the effect of the ground plane dimension. Note that the larger the ground plane is, the better the reflection coefficient is, but the larger ground plane will degrade the omnidirectional property of the proposed antenna. Therefore, both impedance and radiation characteristics should be taken into consideration in choosing an optimized size of the ground plane. When the frequency mode number  $n$  equals 4, Antenna B resonates at 4.4 GHz with the reflection coefficient of better than  $-10$  dB. The other frequency bands ( $n = 2, 3, 5$ ) cover the required band widths of the IEEE 802.11 WLAN standards in the 2.4 GHz, 5.2 GHz and WiMAX in the 3.5 GHz. The comparison of antenna size, resonant frequency and impedance bandwidth between Antenna A and Antenna B is summarized in Table 1.

**Table 1.** The comparison of the Antenna size, resonant frequencies and the impedance bandwidth between the Antenna A and Antenna B. ( $n$  is the frequency mode number).

antenna		Antenna A	Antenna B
parameter			
Size (mm)		$98 \times 20 \times 1$	$28 \times 20 \times 1$
Resonant frequencies (GHz)	$f_1 (n = 1)$	1.12	1.11
	$f_2 (n = 2)$	2.46	2.45
	$f_3 (n = 3)$	3.90	3.55
	$f_4 (n = 4)$	5.42	4.19
	$f_5 (n = 5)$		5.19
Impedance bandwidth (MHz)	$f_1 (n = 1)$	50	
	$f_2 (n = 2)$	180	80
	$f_3 (n = 3)$	320	200
	$f_4 (n = 4)$	300	110
	$f_5 (n = 5)$		180

From Table 1, it is clearly seen that by inserting the spiral structure into the strips of the conventional monopole, the size of the antenna is obviously reduced, and more resonant frequency modes can be excited in the same range of frequency. Compared to Antenna A, Antenna B has the same resonant frequencies at 1.11 GHz and 2.45 GHz while the higher resonant frequencies shift to the lower frequencies, and their impedance bandwidth is reduced. The spiral ring structure provided a shunt capacitance between the outer and inner rings which increase the mode of the input reactance. Thus, the narrowing impedance bandwidth is due to the large fluctuation of the reactance in the range of resonant frequencies.

### 4.2. Studying Effects of the Gap $d$

The effect of the gap  $d$  on the frequency ratio of these multimodal frequencies is studied, and the total length of the spiral ring strips is accordingly adjusted to maintain the fundamental resonance at the same frequency when the gap  $d$  changes. Figure 3 shows the simulated reflection coefficient of Antenna B for different sizes of gap  $d$ . From Figure 3, it can be observed that when the gap  $d$  is increased by a step of 0.5 mm, the first and third resonant frequencies stay the same, and the other three resonant frequencies decrease. The relationship among the other three resonant frequencies is changed due to the variation of the coupling energy between the outer and inner ring strips. Therefore, it is easy to design to an antenna which can meet the required specification of WiMAX and WLAN.

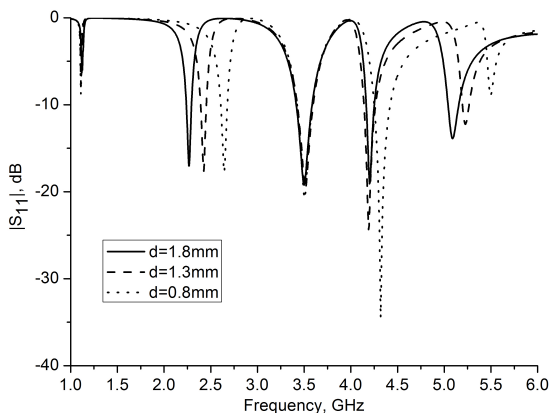


**Figure 3.** Simulated  $|S_{11}|$  of Antenna B with different size of gap  $d$ .

### 4.3. Comparison of Radiation Pattern between Conventional Monopole Antenna and the Proposed Antenna

It is well known that the conventional monopole antenna has multiple frequency modes. However, the higher resonant frequencies cannot be

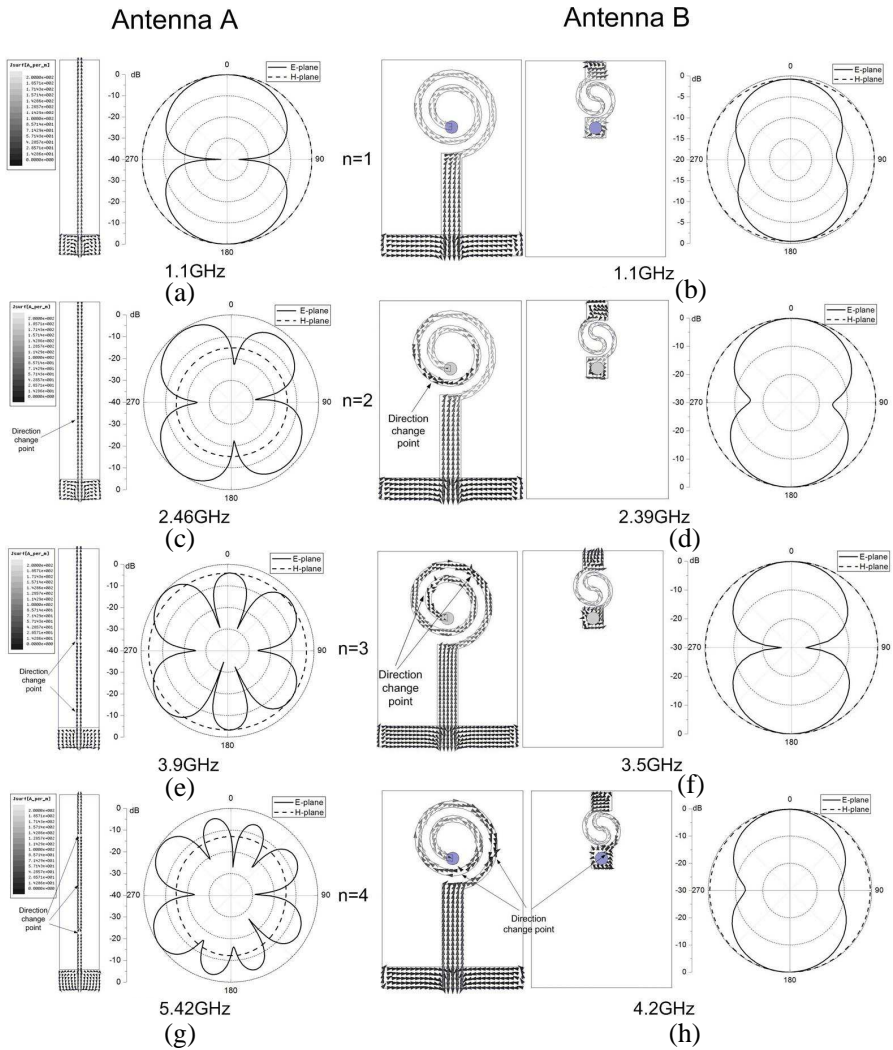


**Figure 4.** Comparison of the surface current distributions and the corresponding radiation patterns between Antenna A and Antenna B at all these multimodal frequencies.

applied to the wireless communication because the radiation patterns at higher operating frequencies are disorderly and unsystematic. By inserting the spiral ring structure into the strip of the conventional monopole, the radiation pattern characteristics at higher operating frequencies are improved. Figure 4 shows comparison of the surface current distributions and the corresponding radiation patterns between Antenna A and Antenna B at all these multimodal frequencies.

From Figures 4(a) and 4(b), we can see that the surface currents on the patch flow in only one direction and that no reverse surface currents contribute to the radiation pattern. Therefore, both the radiation patterns at the fundamental frequency are very good. From Figure 4(c), it is clearly seen that when  $n$  equals 2, the direction of the surface currents on the patch changes one time. With the combined action of the forward and reverse surface currents on the patch, the maximum radiation of Antenna A is not in the direction of the vertical plane but at an angle with it. There are four main lobes in the  $E$ -plane, and the radiated power in the  $H$ -plane decreases a lot, which degrades the performance of the antenna in the wireless communication. Comparing Figure 4(d) with Figure 4(c), we can see that the reverse surface current distributes on the spiral ring strip and that its direction changes with the alteration of spiral structure. Thus, the effect of the reverse current on the radiation pattern can be ignored, and the radiation pattern is mainly contributed by the surface current on the microstrip line. From Figure 4(e) to Figure 4(h), when  $n$  equals 3 or 4, the multi-cycle surface currents distributing on the patch of Antenna A will produce multiple lobes in the radiation pattern which degrades the performance of the antenna. By introducing the spiral structure, the surface current on the microstrip is always in one direction which mainly contributes to the radiation pattern, and the effect of the other surface current is cancelled out in the spiral ring structure. Therefore, the radiation pattern at all these multimodal resonant frequencies can remain stable.

#### 4.4. Comparison of Simulated and Measured Results of the Proposed Antenna

For providing the simulation validation, a prototype based on Antenna B has been fabricated and tested. Figure 5(a) shows the fabricated prototype antenna. The simulated and measured  $|S_{11}|$  of the prototype are compared in Figure 5(b), which exhibit good agreements and meet the  $-10$  dB requirement in most bands. As shown in Figure 5(b), the first band is located at 1.15 GHz with a reflection coefficient of  $-8.4$  dB, which is worse than  $-10$  dB due to the effect of the size of the ground plane. WLAN band in the 2.4 GHz is covered

by the second resonant mode, which extends from 2.4 to 2.5 GHz. The third band stretches from 3.5 to 3.75 GHz, which covers WiMAX in the 3.5 GHz. The fourth band is from 4.1 to 4.2 GHz. Finally, the fifth band, which begins from 5.15 to 5.35 GHz, can also cover the WLAN band in the 5.2 GHz. The measured operating frequency bands are a little higher than the simulated ones due possibly to the small structural fluctuations in the fabrication process.

For the radiation patterns test of the prototype, we have used a standard antenna test set with a horn antenna as a source in an anechoic chamber. Co-polarization and cross-polarization radiation

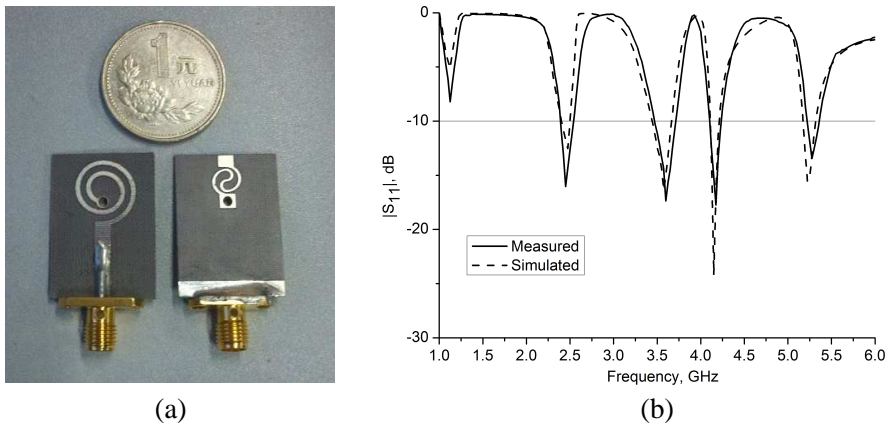


**Figure 5.** (a) The prototype of Antenna B; (b) The measured and simulated  $|S_{11}|$  of the prototype.

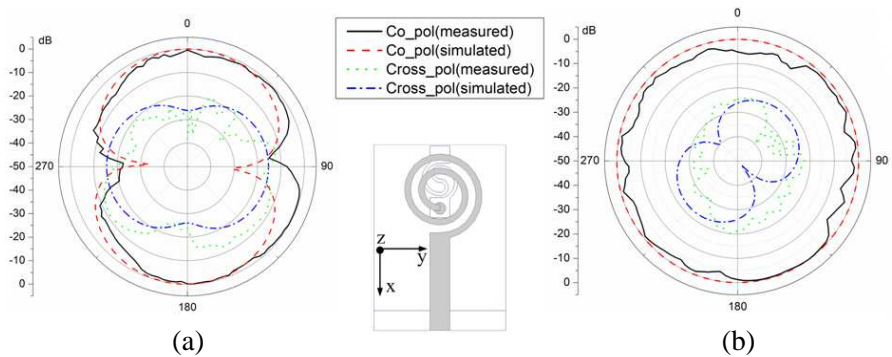


**Figure 6.** The measured and simulated radiation patterns of the prototype at 2.4 GHz. (a)  $E$ -plane; (b)  $H$ -plane.

patterns on  $E$ -plane and  $H$ -plane are exhibited in Figure 6 to Figure 8 for various frequencies. The results show that this proposed antenna has a very good symmetrical figure ‘eight’ radiation in the  $E$ -plane and a very good omnidirectional pattern in  $H$ -plane at all the operating bands. Due to the introduction of the spiral ring radiators at higher frequency bands, the radiation property of the antenna is not degraded.

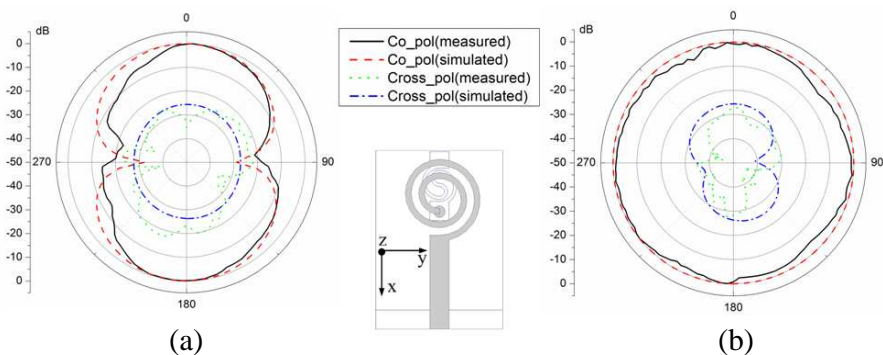


**Figure 7.** The measured and simulated radiation patterns of the prototype at 3.5 GHz. (a)  $E$ -plane; (b)  $H$ -plane.

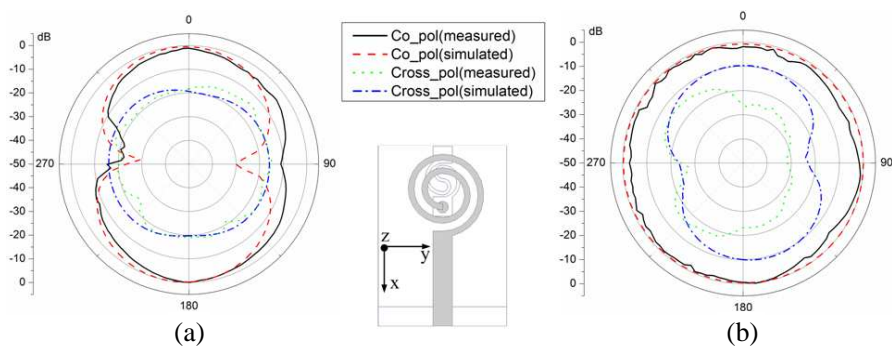


**Figure 8.** The measured and simulated radiation patterns of the prototype at 5.2 GHz. (a)  $E$ -plane; (b)  $H$ -plane.

Finally, the peak antenna gains against frequency for the proposed antenna across these operating bands were measured and shown in Figure 9. As can be found, very stable gain variation across these three operating bands can be achieved. The average gains are about 1.87 dBi (1.84–1.91 dBi) with variation of 0.07 dBi at the 2.4 GHz band, 2.21 dBi (2.15–2.27 dBi) with variation of 0.12 dBi at the 3.5 GHz band,

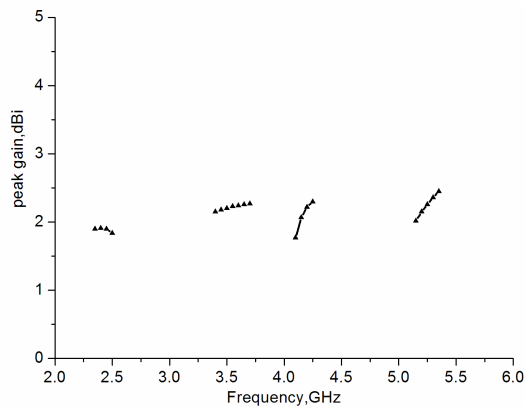


**Figure 9.** The measured peak gains of the prototype.

2.03 dBi (1.77–2.30 dBi) with variation of 0.53 dBi at the 4.2 GHz band, and 2.24 dBi (2.02–2.45 dBi) with variation of 0.43 dBi at the 5.2 GHz band.

## 5. CONCLUSION

A multimode monopole antenna based on spiral ring resonators for improving the radiation pattern is developed in this work. The measured return spectrum complies with the frequency needs of WLAN and WiMAX applications. The proposed antenna design exhibits a compact size of only  $28 \text{ mm} \times 20 \text{ mm} \times 1 \text{ mm}$  and very good radiation patterns at all the resonant frequencies. The frequency ratio of these multimodal frequencies can also be changed. Good impedance matching, monopole-like radiation pattern and stable antenna gains across the operating bands make such an antenna a good candidate in WLAN/WiMAX (2.4/3.5/5.2 GHz) application systems.

## REFERENCES

1. Xiong, J.-P., L. Liu, X. -M. Wang, J. Chen, and Y.-L. Zhao, "Dual-band printed bent slots antenna for WLAN applications," *Journal of Electromagnetic Waves and Applications*, Vol. 22, Nos. 11–12, 1509–1515, 2008.
2. Luo, Y. L. and K. L. Wong, "Printed double-T monopole antenna for 2.4/5.2 GHz dual-band WLAN operations," *IEEE Trans. Antennas Propag.*, Vol. 51, No. 9, 2187–2192, Sep. 2003.

3. Chang, T. N. and J. H. Jiang, "Meandered T-shaped monopole antenna," *IEEE Trans. Antennas Propag.*, Vol. 57, No. 12, 3976–3978, Dec. 2009.
4. Li, Z. Q., C. L. Ruan, L. Peng, and X. H. Wu, "Design of a simple multi-band antenna with a parasitic C-shaped strip," *Journal of Electromagnetic Waves and Applications*, Vol. 24, Nos. 14–15, 1921–1929, Sep. 2010.
5. Lizzi, L. and G. Oliveri, "Hybrid design of a fractal-shaped GSM/UMTS antenna," *Journal of Electromagnetic Waves and Applications*, Vol. 24, Nos. 5–6, 707–719, 2010.
6. Lizzi, L., R. Azaro, G. Oliveri, and A. Massa, "Multiband fractal antenna for wireless communication system for emergency management," *Journal of Electromagnetic Waves and Applications*, Vol. 26, No. 1, 1–11, 2012.
7. Jamalpoor, R., J. Nourinia, and C. Ghobadi, "A wideband microstrip-fed monopole antenna for WiBro, WLAN, DMB and UWB applications," *Journal of Electromagnetic Waves and Applications*, Vol. 22, Nos. 11–12, 1461–1468, 2008.
8. Jaw, J.-L. and J.-K. Chen, "CPW-fed hook-shaped strip antenna for dual wideband operation," *Journal of Electromagnetic Waves and Applications*, Vol. 22, No. 13, 1809–1818, 2008.
9. Jaw, J.-L., F.-S. Chen, and D.-F. Chen, "Compact dual-band CPW-fed slotted patch antenna for 2.4/5 GHz WLAN operation," *Journal of Electromagnetic Waves and Applications*, Vol. 23, Nos. 14–15, 1947–1955, 2009.
10. Pourahmadazar, J., C. Ghobadi, J. Nourinia, and H. Shirzad, "Multiband ring fractal monopole antenna for mobile devices," *IEEE Antennas Wireless Propag. Lett.*, Vol. 9, 863–866, 2010.
11. Ibrahim, A. A., A. M. E. Safwat, and H. El-Hennawy, "Tripe-band microstrip-fed monopole antenna loaded with CRLH unit cell," *IEEE Antennas Wireless Propag. Lett.*, Vol. 10, 1547–1550, 2011.
12. Ban, Y.-L., J.-H. Chen, S.-C. Sun, J. L.-W. Li, and J.-H. Guo, "Printed wideband antenna with chip-capacitor-loaded inductive strip for LTE/GSM/UMTS WWAN wireless USB dongle applications," *Progress In Electromagnetics Research*, Vol. 128, 313–329, 2012.
13. Hsieh, L.-H. and K. Chang, "Simple analysis of the frequency modes for microstrip ring resonators of any general shape and correction of an error in the literature," *Microw. Opt. Technol. Lett.*, Vol. 38, 209–213, 2003.